*Desalination and Water Treatment*
www.deswater.com

doi: 10.1080/19443994.2013.770436

51 (2013) 5873–5885
August

Taylor & Francis
Taylor & Francis Group

# Processing of surface and ground water by hydrostatic pressure-driven membrane techniques: design and economic aspects

Dasari Manjunath, Madupathi Madhumala, Revanur Prasad, Swayampakula Kalyani, Sundergopal Sridhar*

*Membrane Separations Group, Chemical Engineering Division, Indian Institute of Chemical Technology, Hyderabad, 500007, India*
*Tel. +9140 27193408, 27191394; Fax: +9140 27193626; email: s_sridhar@iict.res.in*

Received 29 March 2012; Accepted 23 December 2012

ABSTRACT

In recent years, membrane-based ultrafiltration (UF) and reverse osmosis (RO) have become popular worldwide as possible alternative methods to conventional ion exchange and clarification processes for the production of potable water. The performance of UF and RO membranes was evaluated for treatment of surface and ground water from Prakasam District of Andhra Pradesh, India; namely, jagarlamudi well water (JWW), jagarlamudi pond water (JPW), veerannapalem old pond water (VOPW), and veerannapalem new pond water (VNPW). Pilot-scale UF and RO systems were built indigenously by incorporating commercial hollow fiber polyacrylonitrile UF and thin film composite polyamide RO modules, respectively. Operating parameters such as feed concentration, pressure, and cross-flow velocity were varied to study their effect on membrane performance. Effect of fouling on flux and rejection characteristics of the membrane was evaluated. RO membrane exhibited a rejection of 96.4% for JWW and VOPW feeds with reasonable flux of 42.5 and 48 $L\,m^{-2}\,h^{-1}$, respectively, whereas, UF experiments with JPW and VNPW feeds revealed corresponding turbidity rejections of 95.6 and 98.2%. A mathematical model was developed for commercial RO system to simulate the process for establishing optimum operating conditions. A comparison of UF and RO processes for this application is presented along with useful details of equipment list, process flow diagram of commercial membrane plant, schematic of compact hollow fiber pilot plant, and detailed estimation of operating costs.

*Keywords:* Reverse osmosis; Ultrafiltration; Surface water; Ground water; Mathematical modeling; Economic estimation

## 1. Introduction

Exploitation of water resources is rapidly rising in many regions of the world leading to extensive water scarcity. Demography and human activity are continuously inducing a significant enhancement in water requirements with simultaneous misuse and mismanagement of water resources [1]. Water bodies are being exposed to pollutant contamination from industrial and agricultural activities which affect the maintenance of water resources in a complex way [2]. The phenomena of eutrophication and ecosystem destabilization are currently observed in several countries.

*Corresponding author.

Nevertheless, scientists are developing techniques to conserve water, control drinking water quality through different purification methods, and protect the water environment [3,4].

Conventional treatment processes may not completely remove metabolites and cells of the chlorine-resistant micro-organisms [5]. During the production of potable water, several byproducts may be formed along with dissolved compounds including suspended solids and colloidal particles during the disinfection [6]. Thus, water treated by conventional methods may still contain compounds which are harmful for domestic or industrial application. For these reasons, the raw water used for industrial purposes undergoes additional purification. The removal of suspended solids and colloids can be achieved by using UF [7,8], whereas RO process succeeds in maximum rejection of total dissolved solids (TDS) and organic compounds [9]. For other applications like salt separation or solvent recovery from industrial effluents, Electrodialysis (ED) technology has shown best hydraulic recovery and cost effectiveness compared to other membrane treatment technologies such as RO or UF [10,11]. ED is more economical than RO for desalination of ground water which contains low TDS levels, but becomes increasingly expensive once the TDS concentration becomes higher and goes beyond that of brackish water [12]. Hence, ED is not a cost-effective option for seawater desalination and does not have a barrier effect against microbiological contamination. RO, on the other hand, has the ability to remove all contaminants including excess TDS and harmful microbes in a single step. ED can only remove ionizable compounds such as salts but cannot separate nonionizable species such as natural organic matter which may also be present in the water. While comparing ED with UF, it is worth mentioning that UF can remove both turbidity and harmful microbes from surface water which ED cannot. For surface water, ED needs to be combined with UF to reduce TDS and remove turbidity and microbial content. Alternatively, ED can be combined with UV light treatment to address the issue of microbial contamination.

Many researchers have focused on replacing the conventional pretreatment methods of sand filtration and activated carbon exposure with UF technique, because it offers a stable product water quality and improves compactness of the system [13]. More than 50% of the UF technology is being used globally for treating various water resources including rivers, reservoirs, and lakes [14,15]. In South Africa, the government has aimed at providing the rural and preurban communities with alternative technologies for water purification to replace cumbersome and unsafe conventional water treatment methods [16]. Botes et al. [17] evaluated a UF pilot plant for potable water production, whereas Arnal et al. [18] designed a membrane water potabilization facility to evaluate UF performance. Clever et al. [19] constructed a large-scale pilot plant for the treatment of water coming from the river Weser by a combination of direct ultrafiltration (UF) followed by reverse osmosis (RO) to provide $36\,m^3/h$ of purified water (permeate).

In the present investigation, the collected water samples viz., jagarlamudi well water (JWW), jagarlamudi pond water (JPW), veerannapalem old pond water (VOPW) and veerannapalem new pond water (VNPW), were treated using UF and RO processes. Color, TDS, and turbidity content in the water samples were thoroughly analyzed. With the results obtained, a mathematical model based on statistical mechanical transport equations was developed for commercial RO system. Flux and rejection for a given feed composition at different operating conditions were evaluated. Effect of hydrodynamic operating conditions was studied by varying feed flow rates and the performance of both UF and RO membranes were recorded. Economic estimation of commercial UF and RO systems have been compared by presenting detailed equipment specifications and operating cost calculations. Process flow diagrams for spiral-wound and hollow fiber membrane systems are elucidated.

## 2. Experimental

### 2.1. Materials

Commercial Polyacrylonitrile (PAN) hollow fiber UF module with effective membrane area of 0.8 $m^2$ and thin film composite (TFC) spiral-wound Polyamide RO module with membrane area of $1.0\,m^2$ were procured from Akanksha enterprises, Pune and Permionics Membranes Pvt Ltd., Vadodara, India, respectively. Surface and ground water samples were collected from two villages, Jagarlamudi and Veeranna Palem, in Prakasam District of Andhra Pradesh State, India. Both the surface and ground water bodies contained some fluoride due to hydrogeological conditions, but there was no evidence of any contamination by industrial effluents as proved by detailed water analysis given in Table 1. Citric acid, HCl, EDTA, NaOH, and sodium metabisulphite (SMBS) were obtained from S.D. Fine Chemicals Ltd., Hyderabad, India.

### 2.2. Description of pilot scale RO and UF systems

A pilot-scale skid-mounted system was built incorporating a commercial TFC polyamide RO membrane

Table 1
Characteristics of feed and permeate samples

| Parameters | Water samples | | | | | | | |
|---|---|---|---|---|---|---|---|---|
| | JWW (RO) | | JPW (UF) | | VOPW (RO) | | VNPW (UF) | |
| | Characteristics | | | | | | | |
| | Feed | Permeate | Feed | Permeate | Feed | Permeate | Feed | Permeate |
| TDS (ppm) | 821.1 | 29.59 | 227 | 227 | 502 | 18.52 | 266 | 266 |
| Turbidity (FAU) | 5 | Nil | 46 | 2 | 83 | Nil | 56 | 1 |
| Color (Pt–Co) | 15 | Nil | 48 | 3 | 129 | Nil | 22 | 1 |
| Total hardness (mg/l) | 700 | 40 | 280 | 280 | 480 | 35 | 350 | 350 |
| Total alkalinity (mg/l) | 340 | 20 | 210 | 210 | 280 | 10 | 230 | 230 |
| Calcium (mg/l) | 126 | 10 | – | – | – | – | – | – |
| Magnesium (mg/l) | 90 | 3 | – | – | – | – | – | – |
| Sodium (mg/l) | 120 | 3 | – | – | – | – | – | – |
| Potassium (mg/l) | 2 | <1 | – | – | – | – | – | – |
| Chloride (mg/l) | 250 | 25 | 255 | 255 | 280 | 23 | 260 | 260 |
| Sulfate (mg/l) | 156 | 6 | 170 | 170 | 150 | 3 | 180 | 180 |
| Silica (mg/l) | 18 | 1 | – | – | – | – | – | – |
| Iron (mg/l) | 0.09 | 0.02 | – | – | – | – | – | – |
| Nitrate (mg/l) | 30 | 2 | – | – | – | – | – | – |
| Fluoride (mg/l) | 1.2 | 0.2 | – | – | – | – | – | – |
| COD (mg/l) | <2 | <2 | 120 | <2 | 150 | <2 | 140 | <2 |
| BOD (mg/l) | – | – | 75 | <1 | 80 | <1 | 90 | <1 |
| Total coli forms MPN/100 ml | 1,100 | Nil | 10,000 | Nil | 12,000 | Nil | 9,800 | Nil |

inside a fiber-reinforced plastic cylindrical vessel as shown in Fig. 1. A tank of 50 L capacity made of stainless steel was provided for raw water storage and supplies the feed water to the membrane system. The reject was partially recycled to feed tank and partially disposed through a two-valve arrangement provided on the reject line to recycle part of the reject back to feed tank and dispose the other part. Fresh raw water was added continuously to make up for the decrease in total volume in the feed tank. Hence, the operation was actually carried out in "feed and bleed mode." A high cross-flow velocity of 1,000 L/h of feed flow was maintained to minimize concentration polarization and fouling. A cooling coil was used for circulating cold water to maintain constant ambient feed temperature. A high-pressure pump (Prakash pumps, Vadodara, India) capable of maintaining a pressure up to 2.5 MPa was installed for transporting the feed liquid throughout the system. A polypropylene prefilter rope cartridge of 5 μm pore size was mounted at the upstream side of the spiral membrane module to prevent entry of any suspended solid particles. A restricting needle valve was provided on the concentrate outlet to pressurize the feed liquid to a desired value indicated by a pressure gage installed at a position prior to that of the valve. Permeate and concentrate flow rates were measured using accurately calibrated rotameters containing metal floats. In the UF pilot system, feed was passed through two profilers, namely, micron cartridge and activated carbon filters, to remove sediments, color, chemicals, and odor (Fig. 2). A feed pump capable of maintaining the pressure up to 500 kPa was installed to provide the driving force for mass transfer.

### 2.3. Experimental procedure

Before introducing the feed into the RO system, the membrane was cleaned and wetted with deionized water. Initially, feed water was passed through the prefilter micron cartridge to remove coarse solids. The pretreated water was then pressurized through the membrane using the high-pressure pump. The flow rates of the two streams such as permeate and concentrate streams were measured at regular time intervals using the rotameters. The conductivity and flux values of feed and permeate were recorded as a function of time until the desired water recovery was achieved.

The feed input to the UF system was given through a feed tank of 25 L capacity from where it was passed through the two prefilters, micron cartridge, and activated carbon, which prevent clogging of the hollow fiber membrane. To remove impurities

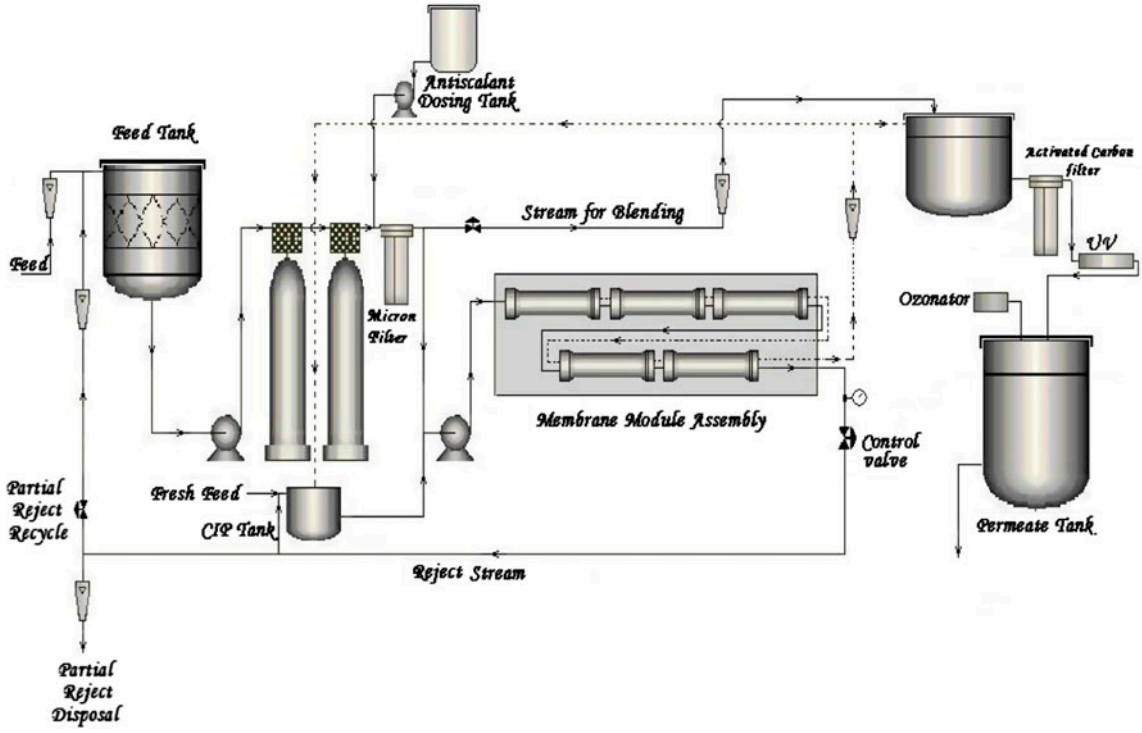


Fig. 1. Schematic process flow diagram of pilot-scale RO system.

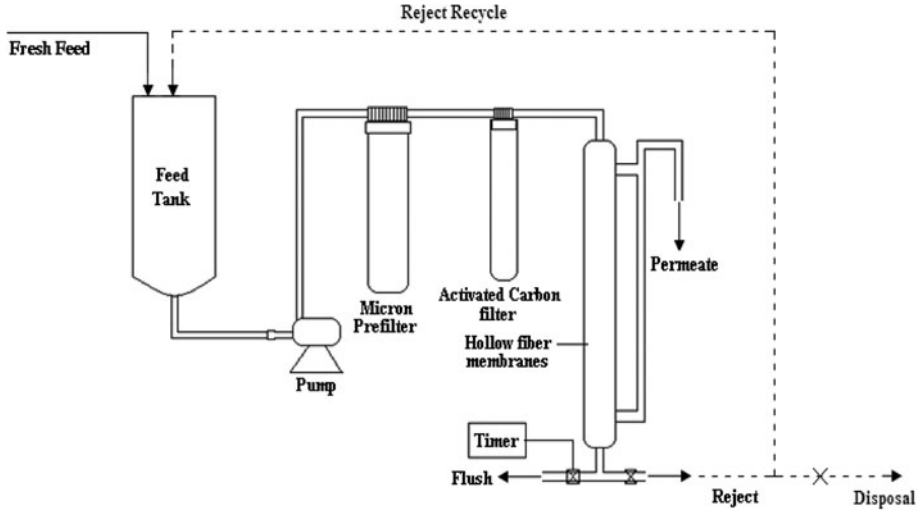


Fig. 2. Schematic process flow diagram of pilot-scale hollow fiber membrane-based UF system.

accumulated inside the fibers, the flush time interval was adjusted using the timer connected to the solenoid valve of the flush line. The reject line valve was adjusted manually for achieving the required recovery. In both type of experiments, the 50% of reject volume was recycled back to the feed tank and remaining part was disposed off.

### 2.4. Membrane fouling and its control

Membrane fouling is caused by suspended solids, microbes, and organic materials present in the feed water that accumulate either on the membrane surface or within the pores. Soluble heavy metals like iron can get oxidized within the modules to form deposits and such similar problems can occur with silica or

even colloidal sulfur [20]. In order to prevent biological fouling by fungus, algae, or microbes, the membrane is stored in sodium metabisulphite (SMBS) aqueous medium (100 g/20L), whereas the removal of mineral scales or metal salt precipitates scales is done using an aqueous solution of citric acid/HCl (1%w/v) which is circulated through the system for 10 min. An aqueous solution containing tetrasodium-EDTA (0.5% w/v) + NaOH (1%w/v) and sodium lauryl sulfate is used for the removal of organic foulants and polishing the surface.

### 2.5. Analytical method

The color and turbidity present in the feed and permeate samples were analyzed using a digital colorimeter (Hach-DR-890, Bangalore, India). The conductivity and pH of the samples were determined by a digital conductivity meter (Model DCM-900, Global electronics, Hyderabad, India) and pH meter (Model DPH-504, Global electronics, Hyderabad, India). The numbers of *Escherichia coli* bacteria present in the samples were estimated by coli form test [21].

## 3. Results and discussion

The characteristics of four different water samples, namely, JWW, JPW, VOPW and VNPW, are given in Table 1. The JPW, VNPW (TDS < 500 ppm) and JWW, VOPW (TDS > 500 ppm) samples were treated using UF and RO systems, respectively. The rejection observed for parameters like turbidity, color, and pH of JPW and VNPW is given in Table 1. Permeate obtained from RO membrane was found to undergo 6 log reductions in *E. coli* bacteria and further processed by UV treatment to produce ultrapure water for drinking. On the other hand, UF process removes microbial content but allows passage of salts present in the feed.

In RO and UF processes, the separation performance of the membrane is denoted in terms of % rejection of TDS and flux ($J$), which are determined as follows [22]:

$$\%R = \left(1 - \frac{C_p}{C_f} \times 100\right) \tag{1}$$

$$J = \frac{V}{A \times t} \tag{2}$$

The osmotic pressure $\Pi$ is given by the following equation:

$$\Pi = n_i C_i \mathrm{RT} \tag{3}$$

Influence of hydrodynamic conditions on RO and UF systems performance was studied by varying the feed flow rate at a constant pressure of 600 kPa and constant feed concentration of 870 ppm. The feed flow rates were adjusted to obtain different values of Reynolds number ($N_{\mathrm{Re}}$) which is defined as:

$$N_{\mathrm{Re}} = \frac{D_H v \rho}{\mu} \tag{4}$$

The following relationships are used to determine $v$ (linear velocity) and $D_H$ (hydraulic diameter) ($D_{\mathrm{H}} = 4\,\mathrm{h}$):

$$\text{Linear Velocity} = \frac{\text{Feed flow rate}}{\text{Flow path area}} \tag{5}$$

and

$$\begin{aligned}\text{Flow path area} = {} & \text{no. of membrane leaves} \\ & \times \text{ length of each leaf} \\ & \times \text{ channel height (h)}\end{aligned} \tag{6}$$

where channel height for spiral modules is usually in the range 0.5–1 mm and the average of 0.75 mm considered for the calculations.

### 3.1. Effect of feed concentration

The effect of feed concentration on flux and% rejection in case of JWW and VOPW is depicted in Table 2. As expected, a rise in the feed concentration results in a decrease influx from 46.47 to 42.58 $\mathrm{L\,m^{-2}\,h^{-1}}$ for JWW and 49.5–48 $\mathrm{L\,m^{-2}\,h^{-1}}$ for VOPW feeds. On other hand, the % rejection increases to a certain point but decreases gradually there after due to concentration polarization and fouling at the membrane surface. Higher solute concentrations at the feed side induce an osmotic pressure gradient which opposes the externally applied pressure gradient. The driving force for the process ($\Delta p$-$\Delta\Pi$) is thus reduced which causes a gradual decrease in flux [23].

### 3.2. Effect of feed flow rate

Studies on influence of hydrodynamic conditions were performed using spiral-wound membrane module of 2 inch dia × 21 inch length by varying the feed flow rates from 10 to 14 L/min. The effect of Reynolds number ($N_{\mathrm{Re}}$) on average flux for both processes and % rejection for RO alone are graphically illustrated in Figs. 3 and 4. From the observations, it can be

Table 2
Experimental results for JWW and VOPW water samples using RO process

| Time of operation (min) | | Feed concentration (ppm) | | % Rejection | | Flux ($L\,m^{-2}\,h^{-1}$) | |
|---|---|---|---|---|---|---|---|
| JWW | VOPW | JWW | VOPW | JWW | VOPW | JWW | VOPW |
| 6 | 5 | 915.2 | 536.72 | 96.99 | 96.72 | 46.47 | 49.5 |
| 12 | 10 | 962.55 | 559.88 | 97.85 | 96.70 | 44.88 | 48.9 |
| 18 | 16 | 1072.95 | 618.5 | 97.29 | 96.65 | 43.91 | 48.5 |
| 24 | 21 | 1,224 | 694.84 | 96.95 | 96.51 | 43.80 | 48.4 |
| 30 | 27 | 1414.8 | 790.4 | 96.5 | 96.38 | 43.59 | 48.4 |
| 37 | 33 | 1,648 | 934.08 | 96.4 | 96.30 | 42.90 | 48.2 |

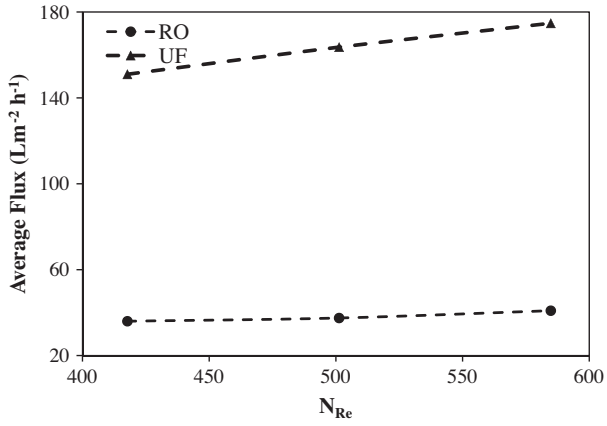


Fig. 3. Effect of Reynold's number ($N_{Re}$) on average flux in RO and UF processes.

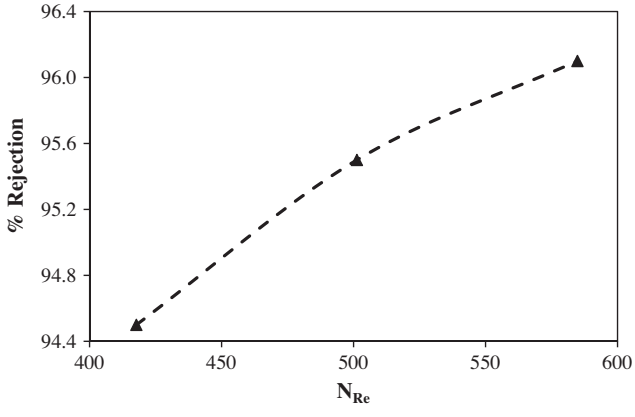


Fig. 4. Effect of Reynold's number ($N_{Re}$) on % rejection in RO process.

observed that as the $N_{Re}$ increased from 417 to 585, the flux was enhanced from 36 to 41 $L\,m^{-2}\,h^{-1}$for RO and 151–174 $L\,m^{-2}\,h^{-1}$in case of UF. On the other hand, the linear velocity for both systems increased from 0.11 to 0.15 $ms^{-1}$over the range of $N_{Re}$ studied.

### 3.3. Development of mathematical model

A mathematical model for RO system (Fig. 5) was developed to calculate the following parameters:

(i) Flux, % rejection, and permeate composition for a given feed composition and operating conditions.
(ii) Prediction of system behavior under varying operating conditions.

### 3.4. RO process model

Mason and Lonsdale (1990) [24] developed the theory, physical assumptions, and range of validity of statistical mechanical model. The basic transport equation for the species $i$ of a multi-component solution is based on the effect of driving force on flux which can be written as:

$$\sum_{j=1}^{N}\frac{c_j}{cD_{ij}}(u_i-u_j)+\frac{u_i}{D_{iM}}=-\frac{1}{RT}\left(\Delta_{T\mu i-F_i}\right)-\alpha_i'B_0/\eta D_{iM}(\Delta p-cF)-\sum_{j=1}^{N}\frac{c_j}{cD_{ij}}D_{ij}^{T}\Delta\ln T \quad (7)$$

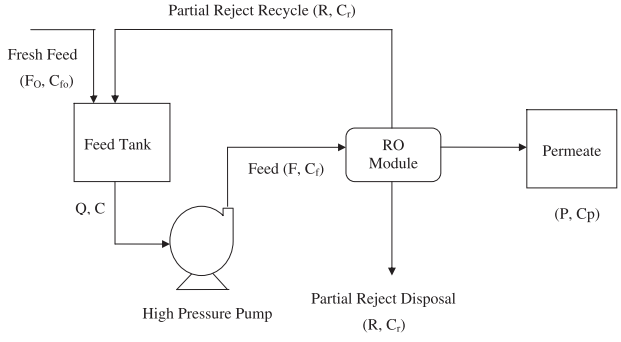


Fig. 5. Schematic of feed and bleed mode of RO operation for simulation study.

On the left-hand side of Eq. (7), two flux-related terms are given, one for solute–solute interaction and one for solute–membrane interaction. On the right hand side, three set of terms appear for the driving forces including isothermal diffusion which depends on concentration, pressure and forced diffusion, viscous (convective) flow, and thermal diffusion.

The above equation is similar to Stefan–Maxwell [12] equation for multi-component diffusion. For binary mixtures, the above equation gives two transport equations, one for each component as given below:

$$\frac{c_2}{cD_{12}}(u_1-u_2)+\frac{u_1}{D_1M}=-\frac{1}{RT}\Delta_{\mu_2}-\frac{\alpha_2' B_0}{\mu D_1 M}\Delta p \tag{8}$$

$$\frac{c_1}{cD_{21}}(u_2-u_1)+\frac{u_2}{D_2M}=-\frac{1}{RT}\Delta_{\mu_2}-\frac{\alpha_2' B_0}{\mu D_2 M}\Delta p \tag{9}$$

(1 and 2 are the solute components present in the solution)

After further simplification

$$J_1=c_1u_1=L_{11}^c\Delta_{\mu 1}-L_{12}^c\Delta_{\mu 2}-\alpha_1 c_1 L_0\Delta_p \tag{10}$$

$$J_2=c_2u_2=L_{21}^c\Delta_{\mu 1}-L_{22}^c\Delta_{\mu 2}\alpha_2 c_2 L_0\Delta_p \tag{11}$$

By changing the component fluxes ($J_1$,$J_2$) to solvent volume flow $J_v$ and solute flux $J_s$ and elaborating the pressure gradients to osmotic pressure gradients $\sigma\pi^a$ and the hydrostatic pressure gradient, we obtain the following set of equations for binary mixtures:

$$J_v\equiv(\bar{V})_1J_1+(\bar{V})_2J_2=-L_p(\Delta p-\sigma_v\Delta\pi^a) \tag{12}$$

$$J_s\equiv-(c_1(\bar{V})_1)\omega\Delta\pi^a+c_2[1-(c_1\bar{V}_1)\sigma_s]J_v \tag{13}$$

For dilute ideal solutions with constant transport coefficients, we have $\sigma_v=\sigma_s=\sigma$, which, therefore, reduces the number of parameters from four to three with ($c_1\bar{V}_1\sim 1$ and $\Delta\pi^a\approx RT(dc_2/d_z)$). The equation for solute flux then becomes:

$$J_s=c_1'(1-\sigma)J_v+\frac{(1-\sigma)J_v(c_2'-c_2'')}{e^{Pe-1}} \tag{14}$$

$$P_e\equiv(1-\sigma)J_v/P \tag{15}$$

$$P\equiv\omega\mathrm{RT}/\Delta z \tag{16}$$

Fractional solute rejection $R$ for RO operation is given by:

$$R\equiv 1-\frac{c_{2''}}{c_{2'}} \tag{17}$$

On further simplification, one obtains:

$$R=\frac{\sigma(e^{Pe-1})}{e^{Pe-\sigma}} \tag{18}$$

$$J_v=\frac{L_p}{\Delta z}\Delta\mathrm{P}_m \tag{19}$$

$$\Delta P_m=\Delta P-\sigma\Delta\pi \tag{20}$$

Using Eq. (15) and (18) and applying power series to$e^{Pe}$, we get

$$\frac{1}{R}=\frac{C_1}{J_v}+C_2 \tag{21}$$

For concentrated solutions,

$$\frac{L_p}{\Delta z}=(D_1C_w+D_2) \tag{22}$$

Therefore $J_v=(D_1C_w+D_2)\Delta P_m$

Due to concentration polarization phenomena caused by selective permeation of solvent, the solute concentration in the membrane interface on the high-pressure side $C_w$ is higher than its concentration in the bulk solution $C_b$. The surface concentration cannot be measured but can be calculated using an Eq. (23) given by Muckenfuss [25].

$$C_w=C_b+(C_b-C_p)(e^{jv/k}-1) \tag{23}$$

Where $k$ is mass transfer coefficient which can be calculated from the available correlation, Sh = $f$(Re, Sc)

According to this theory, $\sigma=R$ which means that Eq. (20) can be written as:

$$\Delta P_m=\Delta P-R\Delta\pi \tag{24}$$

where,

the osmotic pressure

$$\Delta II\ =(C_w-C_p)R_gT \tag{25}$$

$$\Delta P_m=\Delta P-R(C_w-C_p)R_gT \text{ and } C_p=C_w(1-R) \tag{26}$$

Therefore,

$$\Delta P_m=\Delta P-R^2R_gTC_w \tag{27}$$

The developed statistical mechanical model was used to minimize the number of experiments to be performed and also to aid the design of a commercial RO unit. The variation in the pressure, concentration, and mass transfer coefficient of feed and permeate streams along the length of the membrane module can be calculated using this one-dimensional (1D) model. This model can also be extended to a two-dimensional (2D) model, wherein the changes in solute concentrations on feed and permeate side along and across the length of flow could be predicted in order to improve design to achieve better flux and rejection properties. The model could be useful to predict performance of other hydrostatic pressure-driven membrane pilot plants and commercial systems.

### 3.5. Model validation for RO

A statistical mechanical model for spiral-wound RO membrane was developed with the experimental data obtained for JWW sample and the same has been validated to evaluate the accuracy of the model. A comparison of theoretically predicted results with experimental values of reject concentration and % solute rejection is shown in Figs. 6 and 7, respectively, which demonstrates a good agreement with each other at an average of ± 1% deviation. From Fig. 6, it can be concluded that the reject concentration increases with time. Therefore, the flux and % rejection decreases with time (Figs. 7 and 8) due to increase in osmotic pressure and concentration polarization.

From the experimental % R, $J_V$, $C_{P,}$ and $\Delta P$ are obtained, whereas system parameters such as $L_P/\Delta Z$, $C_1$ & $C_2$, and $\Delta P_m$ by neglecting the concentra-

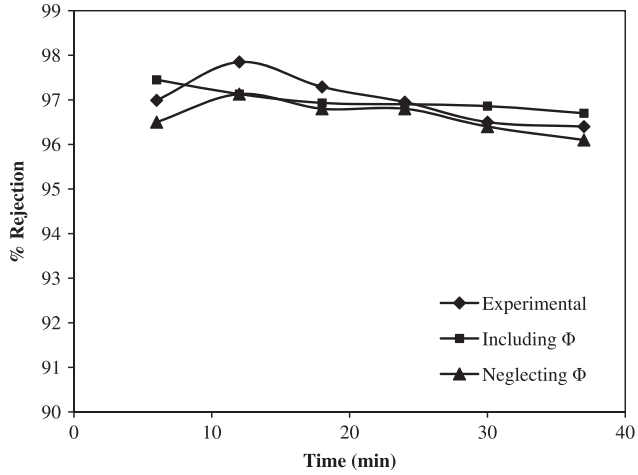


Fig. 7. Comparison of experimental and predicted % rejection with respect to time for JWW feed.

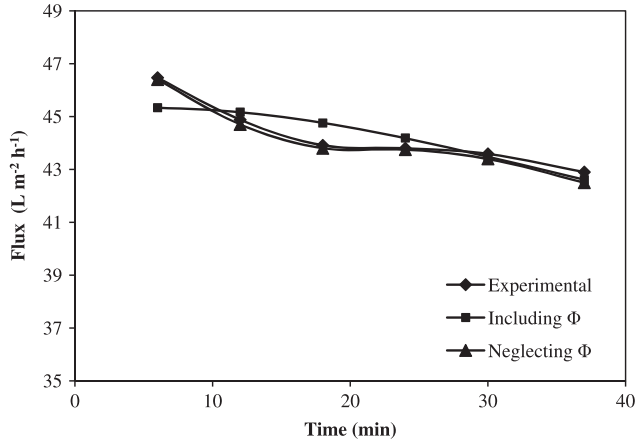


Fig. 8. Comparison of experimental and predicted flux with respect to time for JWW feed.

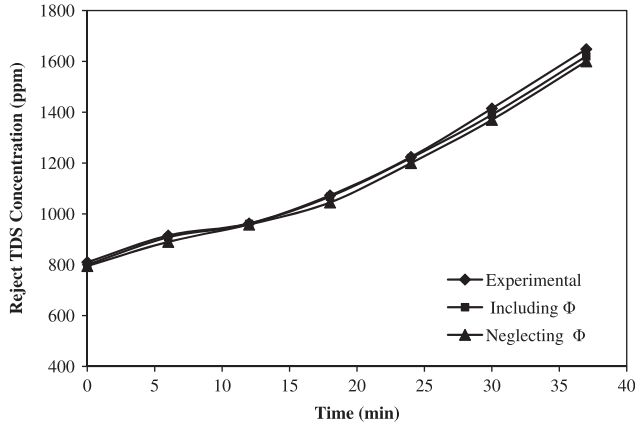


Fig. 6. Comparison of experimental and predicted reject concentration with respect to time for JWW feed.

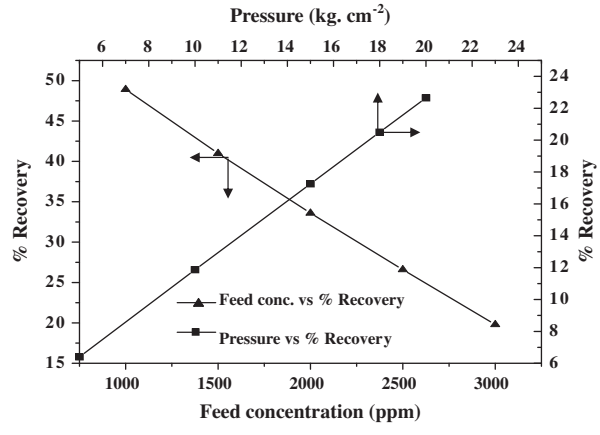


Fig. 9. Effect of feed concentration and feed pressure on % water recovery.

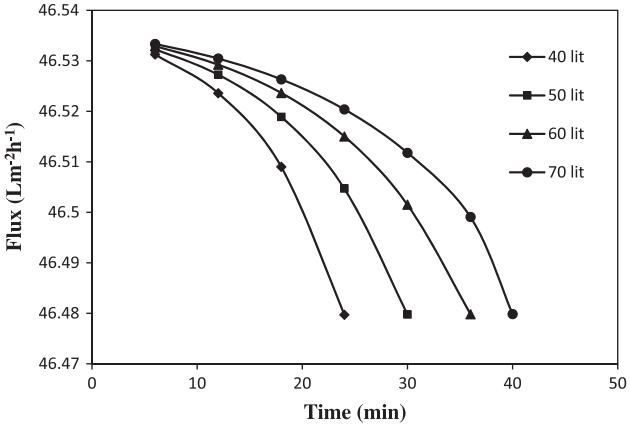


Fig. 10. Effect of operation time on flux for different feed capacities at constant pressure of 650 kPa.

tion polarization were estimated using Eqs. (19), (21), and (24), respectively. A trial and error procedure is followed by assuming an initial guess value of $J_V$ until the error is minimized to 0.001. Similar procedure is followed for determining the system parameters by considering the effect of concentration polarization. An algorithm for simulation assuming the existence of concentration polarization is provided in Appendix-A.

### 3.6. Simulation

In the simulation study, the effect of different operating parameters such as feed concentration, feed pressure, and feed capacity on system performance was investigated. The effect of variation in feed concentration (786 ppm) and applied pressure (650 kPa) on % water recovery is shown in Fig. 9. At various feed capacities, the operation time increases resulting in the decrease of flux (Fig. 10), which is due to the enhancement in reject concentration with time. Simulation was carried out using Matlab-7 software program.

### 3.7. Scale-up and economic estimation

#### 3.7.1. Equipment list and capital cost for RO and UF systems

The list of equipment and corresponding costs for RO and UF systems are given in Table 3, in which the unit price for the major accessories, such as high-pressure pump (Grundfos Company, Chennai, India), TFC Polyamide membrane module with housing, are 1200 USD and 670 USD, respectively. The total capital investment is approximately 3726 USD for the RO system without considering the cost of storage tanks and 920 USD for UF system.

#### 3.7.2. Operation and maintenance cost for RO and UF systems

Operation and maintenance costs of RO and UF systems are given in Table 4, which include module and cartridge replacement cost, power cost, chemical consumption, and cleaning in place (CIP)

Table 3
Equipment lists and capital costs for RO and UF systems

| Item | Capacity/size | MOC | Quantity | Unit Cost (USD) | Total cost | |
|---|---|---|---|---|---|---|
| | | | | | RO | UF |
| 8,040 membrane housing | | – | 1 | 190 | 190 | 190 |
| TFC poly amide membrane modules | (8″dia × 40″long) | – | 1 | 670 | 670 | 300 |
| 1,354 pressure vessel | 35 lpm | – | 1 | 200 | 200 | 120 |
| Skid | 17 lpm | SS | 1 | 200 | 200 | 100 |
| Filter assembly | 35 lpm | PP | 2 | 7.6 | 15.2 | 7.6 |
| Feed pump (2.5HP) | 35 lpm | – | 1 | 116 | 116 | 70 |
| 1 HP high pressure pump | 35 lpm | SS | 1 | 1,200 | 1,200 | |
| 40 Nb TMF (multiport valve) | – | – | 2 | 60 | 120 | |
| Online TDS meter | – | – | 1 | 79 | 79 | 43 |
| Sand & pebbles | – | – | 3 bags | 10 | 30 | 20 |
| Cleaning pump | 2 lpm | SS 316 | 1 | 116 | 116 | |
| 3 phase control panel | – | SS 350/500 | 1 | 170 | 170 | |
| Carbon bags | – | – | 2 | 60 | 120 | 50 |
| Hardware lot | – | – | 1 set | 200 | 200 | 20 |
| UV system | – | – | 1 | 300 | 300 | |
| Total cost | | | | | 3,726 | 920 |

Table 4
Operation and maintenance costs for RO and UF systems

| | RO | UF |
|---|---|---|
| Feed capacity ($m^3$/hr) | 2 | 2 |
| Permeate capacity ($m^3$/hr) | 1.2 | 1.6 |
| Recovery offered | 60% | 80% |
| *Operating cost estimation* | | |
| *Module replacement cost* | | |
| Number of modules (8″dia, 40″long) | 1 | 1 |
| Price per module (USD) | 670 | 300 |
| Total module replacement cost (USD) | 670 | 300 |
| Duration of replacement (Years) | 3 | 3 |
| No. of working hrs/day | 22 | 12 |
| Cost/hr (USD) | 0.028 | 0.023 |
| *Cartridge replacement cost* | | |
| No of cartridges | 3 | 2 |
| Price per cartridge (USD) | 8 | 8 |
| Total cartridge replacement cost (USD) | 24 | 16 |
| Duration of replacement (days) | 180 | 180 |
| No. of working hrs per day | 22 | 12 |
| Cost/h (USD) | 0.006 | 0.0074 |
| *Power cost* | | |
| Feed pump (KW) | 1.12 | 0.372 |
| Dosing systems (KW) | 0.015 | |
| Pump (KW) | 1.85 | 0.372 |
| UV lamp (KW) | 0.072 | 0.072 |
| Total power consumption-KW | 3.057 | 0.817 |
| Hourly cost (USD) (4.5 Rs/unit) | 0.27 | 0.073 |
| Chemical Consumption | | |
| Antiscalant dosing (ppm) | 5 | – |
| Dosage (L/h) | 0.01 | – |
| Cost/lit (USD) | 6.4 | – |
| Hourly cost (USD) | 0.064 | – |
| CIP chemicals (EDTA, NaOH, citric acid) | | |
| Frequency- (days) | 15 | 15 |
| Total cost of CIP per hour-(USD) | 0.045 | 0.045 |
| Total operating cost per hour-(USD) | 0.42 | 0.15 |
| Total operating cost per year assuming 22 & 12 h of operation/day for RO & UF (USD) | 3,356 | 652.6 |
| Depreciation cost (assuming 10% of capital cost) (USD) | 372.6 | 92 |
| Labor cost per year + raw water (USD) | 2,660 | 2,500 |
| Total cost per year (USD) | 6388.6 | 3244.6 |
| *Permeate* | | |
| Quantity (L/h) | 1,200 | 1,600 |
| Operation time (h) | 22 | 12 |
| Quantity of permeate generated in 1 year (L/yr) | 9,636,000 | 7,008,000 |
| Cost/lit of permeate (USD) | $6.63 \times 10^{-4}$ | $4.63 \times 10^{-4}$ |
| If sold at $4 \times 10^{-3}$ USD/lit | | |
| Annual profit (USD) | 32,155 | 24,787 |
| **Pay back period (Yr)** | **0.19** | **0.13** |

chemicals cost. The feed capacity was assumed to be $2\,m^3h^{-1}$, 60% recovery for RO, whereas in case of UF, the corresponding values considered were $2m^3h^{-1}$, feed rate, and 80% recovery. The operation time for RO and UF systems were assumed to be 22 and 12 h per day, respectively. Depreciation costs were taken as 10% of the total capital investment. The life period of hardware is expected to be 10 years, whereas the membrane replacement period is three years.

## 4. Conclusions

To evaluate the feasibility of UF and RO membranes for drinking water production, raw ground and surface water samples were collected from Prakasam district, Andhra Pradesh, India. JWW and VOPW water samples were treated using RO at a constant pressure of 680 kPa and with 60% water recovery, whereas JPW and VNPW samples were treated using UF at a constant pressure of 270 kPa with 80% water recovery. Using the experimental results, a mathematical model based on statistical mechanical transport equations was developed for commercial RO system. Flux, rejection, and permeate composition obtained for given feed composition, capacity, and pressure were predicted. Hydrodynamic operating conditions were varied using bypass valves to study both UF and RO membrane performances. The simulation results obtained exhibited a very good agreement with experimental data at an average deviation of +2%. Economic estimation revealed that UF can be operated at much lower cost than RO for surface water feeds, whereas RO is essential for ground water feeds due the high levels of TDS present in this type of water which cannot be removed by UF. The present RO process model based on a statistical mechanical approach has taken into account all the necessary parameters involved in RO process including osmotic pressure, concentration polarization, and membrane properties like flux and rejection. This model has helped to reduce the number of experiments conducted and most importantly, model validation has shown a fair concurrence with experimental observations.

## Acknowledgments

We are thankful to Council of Scientific and Industrial Research (CSIR) for granting funds for this research work through MATES Network Project under XII Five Year Plan program.

## Nomenclature

| | | |
|---|---|---|
| $C_p$ | — | concentration of solute in permeate |
| $C_f$ | — | concentration of solute in feed |
| $C_w$ | — | concentration of solute at the membrane wall/surface |
| $C_b$ | — | concentration of solute in bulk solution |
| $\Delta\Pi$ | — | osmotic pressure gradient |
| $U_i$ | — | transport velocity of species $i$ |
| $\Delta\_T_\mu 1$ | — | equivalent isothermal gradient of chemical potential of species $i$ |
| $F_i$ | — | external force per mole exerted on species |
| $\Delta P$ | — | total hydrostatic pressure gradient |
| $\Delta P_m$ | — | trans-membrane pressure gradient |
| $D_{ij}$ | — | diffusion coefficient of species $i$ and $j$ within the membrane |
| $D_{iM}$ | — | diffusion coefficient between species $i$ and the membrane |
| $B_O$ | — | viscous flow parameter |
| $H$ | — | viscosity of the solution in the membrane |
| $\alpha_I$ | — | dimensionless parameter |
| $D_{ij}^T$ | — | multi-component thermal diffusion coefficient |
| $L_{ij}^c$ | — | Onsager coefficient in a center of mass frame of reference |
| $L_o$ | — | viscous flow coefficient |
| $\alpha_1$, $\alpha_2$ | — | coefficients that describe viscous separation effects |
| $L_p$ | — | hydraulic conductivity |
| $\omega$ | — | coefficient of solute permeability |
| $\sigma_v$ | — | reflection coefficients for solvent flow |
| $\sigma_s$ | — | reflection coefficient for solute flux |
| $Pe$ | — | Peclet number |
| $P$ | — | solute diffusive permeability |
| $\Delta Z$ | — | effective thickness of the membrane |
| $C_1$ | — | diffusion factor |
| $C_2$ | — | selectivity factor |
| $D_1$ | — | flow factor |
| $D_2$ | — | membrane constant |
| $C_i$ | — | concentration of species i in the solution |
| $n_i$ | — | number of ions present in the solution |
| $R$ | — | universal gas constant ($8.314\,J\,mol^{-1}\,k^{-1}$) |
| $T$ | — | absolute temperature (301 k) |
| $V$ | — | volume of collected permeate (L) |
| $A$ | — | membrane area ($m^2$) |
| $t$ | — | time taken |

## References

[1] B. Watsib, J. Lawrence, Drinking water quality and sustainability, Water Qual. Res. J. Can. 38 (2003) 3–13.
[2] A.H. Mahvi, J. Nouri, A.A. Babaaei, R. Nabizadh, Agricultural activities impact on groundwater nitrate pollution, J. Environ. Sci. Technol. 2 (2005) 41–47.

[3] K. Ijeoma, O.K. Achi, Industrial effluents and their impact on water quality of receiving rivers in Nigeria, J. Appl. Technol. Environ. Sanit. 1 (2011) 75–86.
[4] J. Drok, Z. Koncan, Estimation of sources of total phosphorous in a river basin and assessment of alternatives for river pollution reduction, Environ. Int. 28 (2002) 393–400.
[5] K. Karakulski, M. Gryta, A. Morawski, Membrane processes used for potable water quality improvement, Desalination 145 (2002) 315–319.
[6] J.Q. Jiang, B. Lloyd, A review—Progress in the development and use of ferrate(VI) salt as an oxidant and coagulant for water and wastewater treatment, Water Res. 36 (2002) 1397–1408.
[7] A.B.F. Grose, A.J. Smith, A. Donn, J.O. Donnell, D. Welch, Supplying high quality drinking water to remote communities in Scotland, Desalination 117 (1998) 107–117.
[8] O. Lorain, B. Hersant, F. Persin, A. Grasmick, N. Brunard, M. J. Espenana, Ultrafiltration membrane pre-treatment benefits for reverse osmosis process in seawater desalting. Quantification in terms of capital investment cost and operating cost reduction, Desalination 203(3) (2007) 277–285.
[9] K. Karakulski, M. Grytaand, A. Morawski, Pilot plant studies on the removal of trihalomethanes by composite reverse osmosis membranes, Desalination 140 (2001) 227–234.
[10] AWWA Committee report: Current perspectives on residual management for desalting membranes, J. AWWA 96 (2004) 73–87.
[11] S.A. Kalogirou, Seawater desalination using renewable energy sources, Prog. Energy Combust. Sci. 31 (2005) 242–281.
[12] R. Rautenbach, R. Albert, Membrane Processes, Wiley, Chichester, 1989.
[13] A. Jafarian, L. Abkar, M. Bonakdar, M. Saffari, Ultra-nano filtration: A promising practice to supply potable water from surface resources, Water Pract. Technol. 5 (2010) 1–8.
[14] Z.V.P. Murthy, L.B. Chaudhari, Treatment of distillery spent wash by combined UF and RO processes, Global Nest J. 11 (2009) 235–240.
[15] J.M. Laine, D. Vial, P. Moulart, Status of after 10 years of operation- overview of UF technology today, Desalination 13 (1) (2000) 17–25.
[16] Xia. Sheng-ji, Liu. Ya-nan, Li. Xing, Yao. Juan-juan, Drinking water production by ultrafiltration of Songhuajiang river with PAC adsorption, *J. Environ. Sci*. 19 (2007) 536–539.
[17] J.P. Botes, E.P. Jacobs, S.M. Bradshaw, Long-term evaluation of a UF pilot plant for potable water production, Desalination 115 (1998) 229–238.
[18] J.M. Arnal, M.S. Fern´andez, G.V. Martın, Design and construction of a water potabilization membrane facility and its application to the third world countries, preliminary tests, Desalination 145 (2002) 305–308.
[19] M. Clever, F. Jordt, R. Knauf, N. Raebiger, M. Rtidebusch, R. Hilker-Scheibel, Process water production from river water by ultrafiltration and reverse osmosis, Desalination 131 (2000) 325–336.
[20] J. Kucera, Properly apply reverse osmosis, Chem. Eng. Prog. 93 (1997) 54–61.
[21] A.D. Eaton, L.S. Clesceri, A.E. Greenberg, M.A.H. Franson, American Public Health Association, Standard Methods for the Examination of Water and Wastewater, 20th ed., APHA, Washington, DC, 1998.
[22] G. Owen, M. Bandi, J.A. Howell, S.J. Churchouse, Economic assessment of membrane processes for water and wastewater treatment, J. Membr. Sci. 102 (1995) 77–91.
[23] B.L. Pangarkar, M.G. Sane, M. Guddad, Reverse osmosis and membrane distillation for desalination of groundwater: A review, ISRN. Mater. Sci. 2011 (2011) 1–9.
[24] E.A. Mason, H.K. Lonsdale, Statistical-mechanical theory of membrane transport-A review, J. Membr. Sci. 51 (1990) 1–81.
[25] C. Muckenfuss, Stefan–Maxwell relations for multicomponent diffusion and the Chapman Enskog solution of the Boltzmann equations, J. Chem. Phys. 59 (1973) 1747–1752.

**Appendix A: algorithm for simulation assuming existence of concentration polarization (ϕ)**

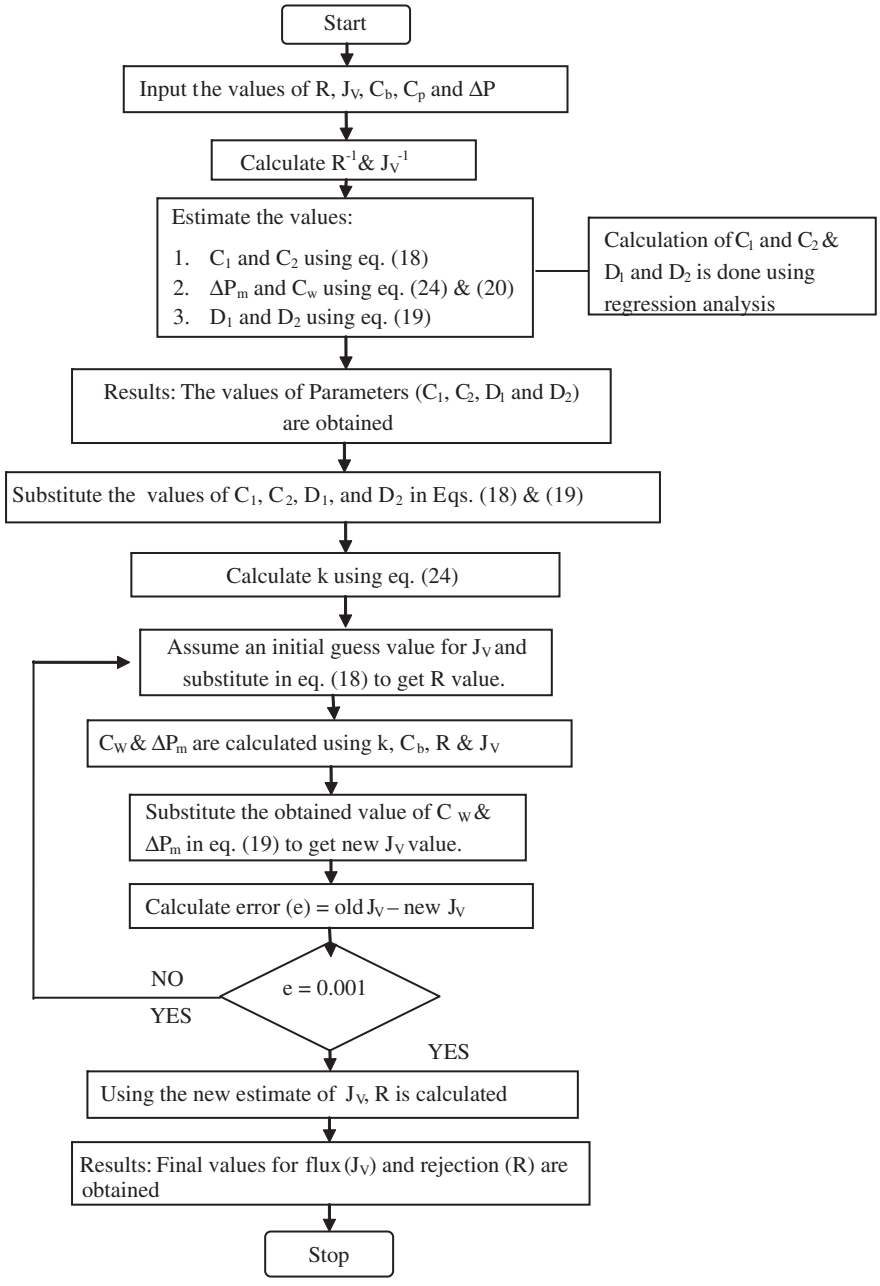


After calculation of rejection and flux, feed concentration can be calculated using material balance equations given below:

Feed input to the RO module = Quantity of Permeate Collected + Amount of Recyled Rejecti.e $F = R + P$

Feed balance:

$$Q(t) = Q(0) - [J \times \text{area} \times \text{time}] \quad (28)$$

Solute balance:

$$Q(t)C(t) = Q(0)C(0) - [J \times \text{area} \times \text{time} \times C_p] \quad (29)$$

Using Eqs. (25) and (26), we can calculate concentration as a function of time and duration for total operation can also be found.